

# Distribution pattern of potential fishing zones in the Bangka Strait Waters: An application of the remote sensing technique

*by Fauziah Fauziah*

---

**Submission date:** 12-Dec-2021 06:45AM (UTC+0700)

**Submission ID:** 1727791382

**File name:** 01Fauziah\_2021\_EJRS-D-21-00158\_Final.docx (3.97M)

**Word count:** 5208

**Character count:** 29168

1 **Distribution pattern of potential fishing zones in the Bangka Strait Waters:**

2 **An application of the remote sensing technique**

3 Fauziyah\*, Agung Setiawan, Fitri Agustriani, Rozirwan, Melki, Ellis Nurjuliasti Ningsih, T  
4 Zia Ulqodry

5  
6 Marine Science Department, Faculty of Mathematics and Natural Sciences, Sriwijaya  
7 University.

8 Jl. Raya Palembang - Prabumulih KM. 32, Indralaya, Ogan Ilir Regency, Province of South  
9 Sumatra, postal code 30862, Indonesia

10  
11 \*Corresponding Author: Email: [siti\\_fauziyah@yahoo.com](mailto:siti_fauziyah@yahoo.com); [Fauziyah@unsri.ac.id](mailto:Fauziyah@unsri.ac.id)

12  
13 **Abstract.** Information regarding fishing grounds was needed to assist fishermen in their fishing  
14 activities. Information about the sea surface chlorophyll-a concentration (SSCC) and sea  
15 surface temperature (SST) could be used as a reference to identify potential fishing zones (PFZ).  
16 The purpose of this study was to identify SST and SSCC data using MODIS (Moderate  
17 Resolution Imaging Spectroradiometer) satellite imagery for determining the PFZ and  
18 analyzing their distribution pattern seasonally. The determination of the PFZ point was carried  
19 out by overlaying the SSCC and SST data based on the results of image data processing. The  
20 results showed that the distribution pattern of PFZ points in the Bangka Strait waters was  
21 predominantly found in the Banyuasin waters. The distribution pattern of PFZ points in the dry  
22 **season (June-August) and transition season II (September-November)** had the same pattern and  
23 tended to dominate the coastal areas of the waters. The distribution patterns in the wet season  
24 (December-February) and transition season I (March-May) spread throughout the Bangka Strait  
25 waters. The most PFZ points were found in transition season I (636 PFZ points), while the  
26 minor PFZ points were found in transition season II (219 PFZ points). Integrating the remote  
27 sensing and GIS technique with statistical validation tests were useful and became a simple

28 method for identifying the PFZ distribution. However, validating the PFZ distributions using  
29 the catch data was required.

30 **Keywords:** chlorophyll-a, GIS, MODIS, sea surface temperature, seasonal variability

31

## 32 **1. Introduction**

33 The Bangka Strait waters are waters that separate the Sumatra and Bangka islands. These  
34 waters have an area of 11,543,142 km<sup>2</sup> and have become the center of fishing activities for  
35 fishermen from Banyuasin and Ogan Komering Ilir Regency of the South Sumatra province as  
36 well as the South Bangka Regency of the Bangka-Belitung province. Based on the capture  
37 fisheries statistics data, the catch production from the Banyuasin regency has drastically  
38 increased from 5,479 tons in 2017 to 64,587 tons in 2019. The catch production from the South  
39 Bangka Regency has also increased from 37,382 tons in 2017 to 38.867 tons in 2019. On the  
40 contrary, decreasing in catch production occurred in Ogan Komering Ilir Regency, where the  
41 decline in production was probably due to climatic factors.

42 The changes in the sea surface chlorophyll-a concentration (SSCC) and sea surface  
43 temperature (SST) are the most critical parameters that used for identifying fish availability and  
44 abundance of the pelagic species (Fitrianah et al., 2016b; Karuppasamy et al., 2020) as well as  
45 considered for estimating potential fishing zones (PFZ) (Fitrianah et al., 2016a; Guidetti et al.,  
46 2010; Nammalwar et al., 2013). Both parameters synergistically influence marine biota  
47 availability, ranging from plankton to marine mammals (Karuppasamy et al., 2020; Rajagopal  
48 et al., 2010). The SST and other environmental factors (pH, oxygen, salinity) would covary  
49 depending on the region characteristics. For different environments variables, there are different  
50 characteristics for determining the PFZ (Fitrianah et al., 2016b). Additionally, SSCC is a proxy  
51 for phytoplankton biomass and is used to identify habitats of fish resources (Karuppasamy et  
52 al., 2020; Nurdin et al., 2015; O'Reilly et al., 1998). The PFZ is a short-term prediction and

53 credible on the zone of fishes aggregation in the open sea (Subramanian et al., 2014). It also  
54 explained that the PFZ is the zone where the fishes aggregate due to a food abundance. Their  
55 availability is limited by this zone in the open sea, where a sharp SST gradient with optimal  
56 SSCC co-occurrence at a given period. (Giri et al., 2016). Appropriately estimating the PFZ  
57 can optimize the fishing operation schedule (Nammalwar et al., 2013).

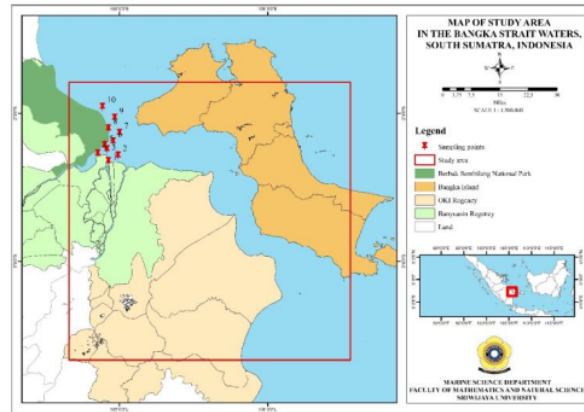
58 In recent decades, the utilization of <sup>4</sup> remote sensing technology and geographic information  
59 systems (GIS) have been conducted to analyze SSCC and SST for estimating the PFZ (Devi et  
60 al., 2015; Harahap et al., 2020; Suhadha and Asriningrum, 2020) as well as for identifying the  
61 distribution patterns of fish and their interactions with other factors (Mustasim et al., 2015).  
62 MODIS algorithms have been of greater value for oceanographic data extraction (e.g., SST and  
63 SSCC data). Using in-situ data helps test the PFZ validity (Ardianto et al., 2017; Daqamseh et  
64 al., 2019). This present research identified PFZ's and analyzed their distribution pattern using  
65 MODIS data for three years (2017- 2019).

66

## 67 <sup>2</sup> 2. Materials and Methods

### 68 2.1 Study Area

69 The study area and <sup>2</sup> sampling location are illustrated in Fig. 1. Besides the main maritime  
70 gateway for South Sumatra, the Bangka Strait waters are also a significant fishing ground,  
71 especially for fishermen from the Banyuasin, Ogan Komering Ilir (OKI), and South Bangka  
72 Regency. These waters are categorized into the Indonesian Fisheries Management Area 711  
73 (WPPNRI-711). The oceanographic conditions in these waters are influenced by the monsoon  
74 and tide cycle. Most fishing activities from South Sumatra that operated in the Bangka Strait  
75 include small-scale fisheries. The Banyuasin waters are strongly affected by the Musi River  
76 run-off (Fauziyah et al., 2019).



77

78 **Fig. 1.** Map of the study area and sampling points in the Bangka Strait waters.

79

## 80 2.2 Data Collection

81 The satellite data used in this study were SST and SSCC monthly data derived from level-  
 82 3 MODIS satellite imagery for three years (2017-2019) with a resolution of 4 km. Besides  
 83 providing monthly data, this level-3 data also provides daily, weekly and yearly data (Suhadha  
 84 and Asriningrum, 2020). Images data were <sup>7</sup> downloaded from the [oceancolor.gsfc.nasa.gov](http://oceancolor.gsfc.nasa.gov)  
 85 website using the Aqua MODIS Chlorophyll Concentration OCI Algorithm sensor and the  
 86 Aqua MODIS Sea Surface Temperature (11 day time). Image data collection and processing  
 87 were carried out in the Remote Sensing Laboratory and Marine Geographic Information  
 88 System, Faculty of Mathematics and Natural Sciences, Sriwijaya University.

89 The PFZ parameter (SSCC and SST data) derived from the MODIS data would be validated  
 90 using field data. The field data collection was carried out on October 24-28, 2020.  
 91 Determination of the sampling locations was carried out using the purposive sampling methods  
 92 by considering the conditions and characteristics of the coastal waters around the Berbak  
 93 Sembilang National Park (BSNP). In this study, ten sampling locations were taken. Each  
 94 location point was recorded in its geographic position on the device (GPS). Chlorophyll-a water  
 95 samples were taken directly by using a water sampler on the sea surface with one repetition,

96 were then put into the sample bottle. Measurement of sea surface temperature parameters was  
97 carried out using the Water Quality Checker.

## 98 2.3 Data Analysis

### 99 2.3.1. Identifying SSCC and SST from the MODIS data

100 After collecting the level-3 data, image data processing used SeaDAS 7.4 software,  
101 Microsoft Excel, and ArcGIS 10.5. Image processing steps include image cropping, NaN  
102 correction, interpolation, contouring SST and SSCC, overlay, and determining PFZ points.  
103 Image cropping was done to make the observed area easier to analyze and reduce the image  
104 storage size. NaN data is the result of reflection from objects that are not numerically detected  
105 by satellite imagery. Meanwhile, interpolation is performed to predict unknown values by using  
106 known values around them. Contouring SST and SSCC were carried out using the contour tools  
107 on ArcMap. SST is used to identify the thermal front zone indicated by a temperature gradient  
108 of 0.5°C (Ardianto et al., 2017; Hasyim et al., 2009). Meanwhile, SSCC selected data to identify  
109 PFZ is 0.2-0.5 mg/m<sup>3</sup> (Ardianto et al., 2017; Suhadha and Asriningrum, 2020).

110 The SST MODIS data for daytime are generated based on the following algorithm (Brown  
111 and Minnett, 1999):

$$112 \quad SST = c_1 + c_2 * T_{11} + c_3 * (T_{3132}) * T_{src} + c_4 * (\sec(\theta) - 1) * (T_{3132})$$

113 where  $T_{31}$  and  $T_{32}$  are the brightness temperatures measured in bands 31 and 32,  $\theta$  is the satellite  
114 zenith angle measured at the sea surface, as well as  $c_1$ ,  $c_2$ ,  $c_3$ , and  $c_4$  are the coefficients whose  
115 values are determined depending on the difference  $T_{31}-T_{32}$ . Meanwhile, the SSCC MODIS data

116 are processed based on the OC3M algorithm (O'Reilly et al., 2000):

$$117 \quad Chl_a = 10^{0.283-2.753R+1.457R^2+0.659R^3-1.403R^4}$$

$$118 \quad R = \log_{10} \left( \frac{Rrs(442)}{Rrs(550)} > \frac{Rrs(490)}{Rrs(550)} \right)$$

119 where  $Chl_a$  is the chlorophyll-a concentration in  $mg.m^{-3}$ ,  $Rrs$  is the remote sensing reflectance,  
120 and  $R$  is the reflectance ratio. The SeaDAS software version 7.4 was used to process and analyze  
121 the MODIS SST and Chl-a datasets.

### 122 2.3.2. Analyzing in-situ data

123 The SST data obtained from measurements using the Water Quality Checker were  
124 tabulated according to the sampling sites. For calculating the SSCC based on  
125 spectrophotometric analysis, the following formulas were used (Aminot and Rey, 2001; Johan  
126 et al., 2014):

$$127 \quad Chl_a(\mu g/L) = (11.86 \times E_{664}) - (1.54 \times E_{647}) - (0.08 \times E_{630}) \dots \dots \dots (1)$$

$$128 \quad Concentration\ of\ Chl_a(mg/L) = \frac{[Chl_a \times v]}{V \times L} \dots \dots \dots (2)$$

129 Where  $v$  is acetone extraction volume (10 mL),  $V$  is filtered volume (500 mL),  $L$  is cuvette light-  
130 path (cm),  $E_{664}$  is absorbance value at wavelength 664 nm,  $E_{647}$  is absorbance value at  
131 wavelength 647 nm, and  $E_{630}$  is Absorbance value at wavelength 630 nm.

### 132 2.3.3. Validating MODIS data

133 The multiple linear regression model could be developed to validate the SST and SSCC  
134 data from the Image Data Processing against in-situ data measurements (Daqamseh et al.,  
135 2019). The linear relation was applied for determining the best-fitted model. In addition, the  
136 RMSE-observations Standard Deviation Ratio (RSR) and determination coefficient ( $R^2$ ) were  
137 used as statistical parameters for the model validation (Fauziyah et al., 2020). For validating  
138 the MODIS data, the MODIS SSCC and SST data on October 2020 closest to the sampling  
139 stations were selected.

### 140 2.3.4. Identifying PFZ

141 An overlay was done by combining the contour of SST and SSCC using the Intersect tool  
142 on the Geoprocessing bar, in which the output was converted into a point to produce a PFZ

143 point. The results of the PFZ map will be made monthly data and grouped seasonally referring  
144 to a fishing season (Fauziyah et al., 2018), namely the wet season (December-February), the  
145 transitional season I (March-May), the dry season (June-August), and the transitional season II  
146 (September-November).

147

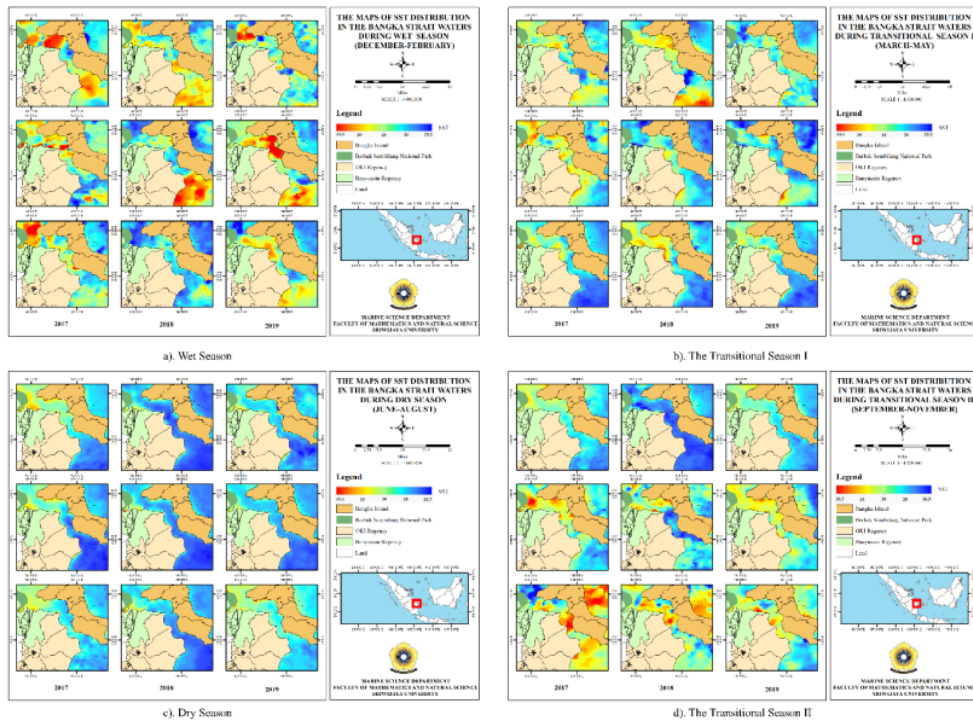
### 148 **3. Result and Discussion**

#### 149 *3.1 Distribution of Sea Surface Temperature (SST)*

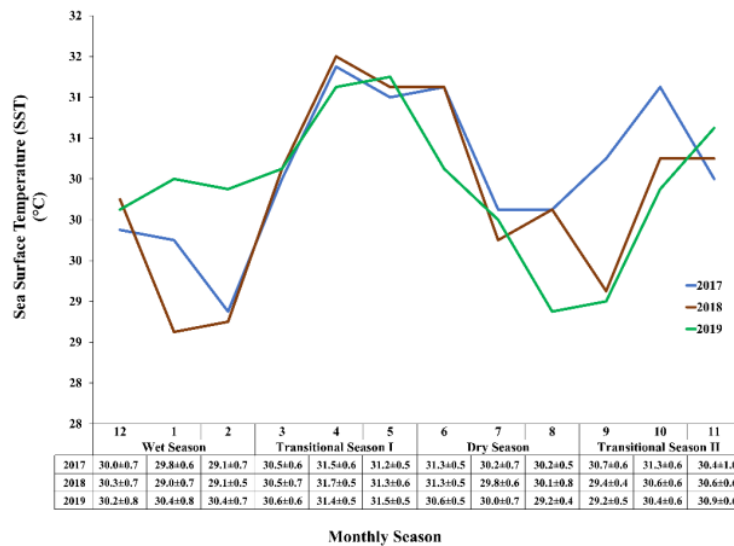
150 The SST distribution map for three years (2017-2019) was analyzed and displayed (Fig. 2  
151 and 3). The SST explains a suitable marine environment for PFZ. In the wet season (Fig. 2a),  
152 the SST values ranged from 25.2-35.5 °C, with the SST mean gone from 28.9-30.4 °C (Fig. 3).  
153 Visually showed that warm temperatures tend to be in the northern part in the waters of Bangka  
154 Strait, and cold temperatures are seen in the southern region in the waters of Bangka Strait.  
155 Still, this condition did not show a regular pattern. Entering transition season I (Fig. 2b), the  
156 SST value in the waters of the Bangka Strait ranged from 28.2-36.2 °C and was visually  
157 distributed throughout these waters. These waters tend to be stable, and their SST distribution  
158 pattern was evenly distributed and had almost the same pattern from 2017 to 2019, with the  
159 SST mean ranging from 30.4–31.6 °C (Fig. 3). Compared to the wet season, the transitional  
160 season I have a higher SST average, and a difference in the movement of SST with the wet  
161 season was seen. In the dry season (Fig. 2c), the SST values ranged from 25.7–35.1 °C, with  
162 the SST mean values ranging from 29.1–31.3 °C (Fig. 3). Visually warm temperatures were  
163 seen in the northern part of the waters of the Bangka Strait and tended to approach the coastal  
164 waters of Banyuasin. Cold temperatures tend to be in the southern part of the waters of the  
165 Bangka Strait. Entering the transitional season II (Fig. 2d), the SST values ranged from 26.9–  
166 35.7 °C, with the SST mean values ranging from 29.2–31.3 °C (Fig. 3).



167        The SST distribution pattern in the waters of the Bangka Strait showed that temperatures  
168        were increasing from September to November. Still, in September, cold temperatures were seen  
169        in the southern part, and warm temperatures were in the northern part of the waters of the  
170        Bangka Strait. In the wet season (Fig. 2a), there was a quite significant fluctuation entering  
171        transitional season I. This is because the rainfall is getting lower in this season so that the sea  
172        surface temperature begins to stabilize and has an optimum SST value, which can affect a good  
173        fishing area. Entering the dry season and transition season II, the SST fluctuations tend to be  
174        unstable but have almost the same pattern.



175 **Fig. 2.** The maps of SST distribution: a) Wet Season (December-February); b) Transitional  
 176 Season I (March-May); c) Dry Season (June-August); d) Transitional Season II  
 177 (September-November)



178 **Fig. 3.** Graph of fluctuation in the average distribution of sea surface temperature in the  
 179 waters of the Bangka Strait

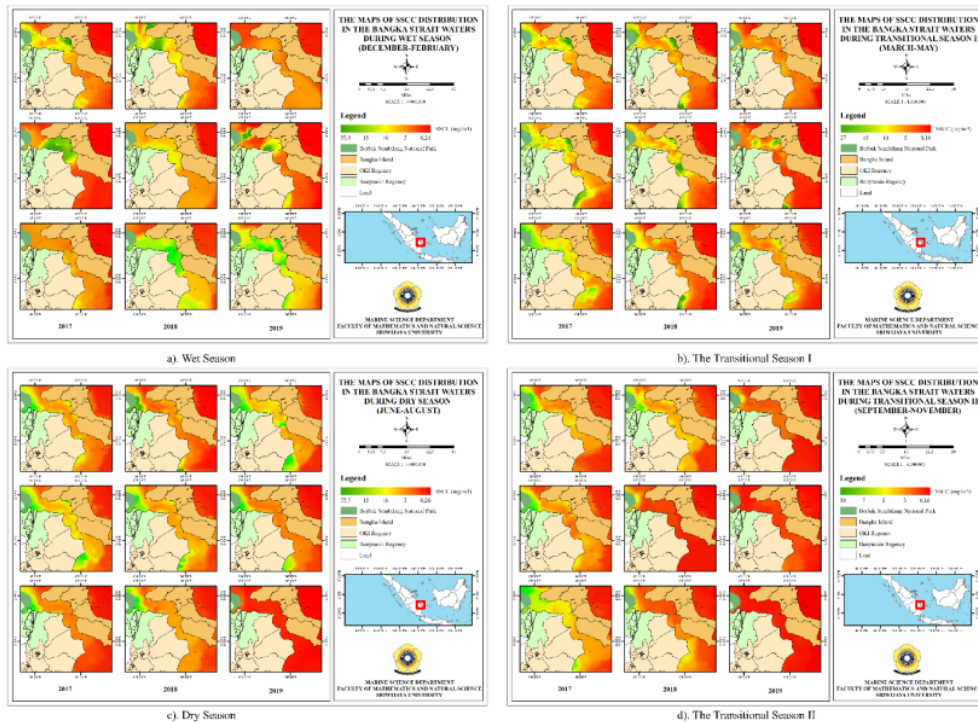
180

181 Overall, the fluctuation of SST values during three years showed the same pattern (Fig. 3).  
182 This results in line with the SST distribution pattern that occurred in the northern waters of  
183 West Java (Harahap et al., 2020). During the transitional seasons, the high-SST values are  
184 affected by rainfall, wind speed, sea surface current, and the sun's daily motion (Harahap et al.,  
185 2020). In this study, the SST mean was highest in <sup>5</sup> transition season I, and this result was similar  
186 to the SST characteristics of Indonesian waters (Marini and Setiawan, 2018).

187 <sup>4</sup> 3.2 Distribution of sea surface chlorophyll-a concentration (SSCC)

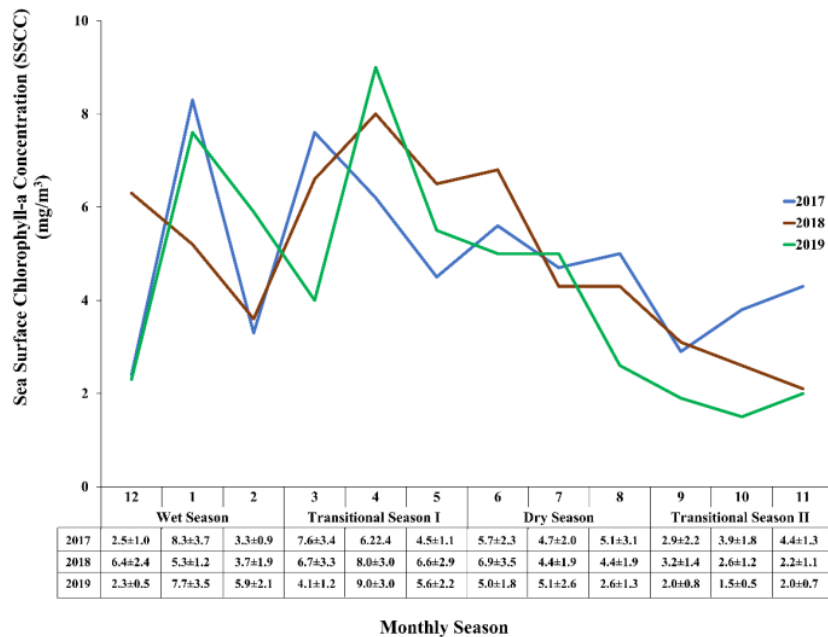
188 The SSCC distribution map for three years (2017-2019) was analyzed and displayed (Fig.  
189 4 and 5). Similar to the TSS distribution, the SSCC distribution also plays an essential role in  
190 determining PFZ. In the wet season (Fig. 4a), the SSCC value ranged from 0.24-35.4 mg/m<sup>3</sup>,  
191 while the SSCC mean values ranged from 2.3-8.3 mg/m<sup>3</sup> (Fig. 5). Visually, the highest SSCC  
192 value was seen in the middle of the Bangka Strait waters, and the lowest SSCC value tends to  
193 be in the southern part of the Bangka Strait waters. The distribution pattern of SSCC for three  
194 years appears to have the same distribution pattern. Entering transition season I (Fig. 4b), the  
195 SSCC values in the Bangka Strait waters ranged from 0.16-27 mg/m<sup>3</sup>, with the SSCC mean  
196 ranging from 4.0-9.0 mg/m<sup>3</sup> (Fig. 5). Their mean values in this season slightly increased than  
197 in the wet season. Visually, it shows that the SSCC values tend to be evenly distributed  
198 throughout the Bangka Strait waters. Their distribution pattern tends to be higher in the coastal  
199 part of the Bangka Strait waters and forms a water mass pocket on the coastal part of Bangka  
200 waters. The dry season (Fig. 4c) ranged from 0.26-22.5 mg/m<sup>3</sup>, while the SSCC mean values  
201 ranged from 2.6-6.8 mg/m<sup>3</sup> (Fig. 5). Visually, their distribution pattern tends to be in the coastal  
202 part of Banyuasin waters. The high SSCC values in Banyuasin waters were thought of since  
203 several large estuaries as nutrient inputs from land affect their high values in Banyuasin waters.  
204 Entering transition season II (Fig. 4d), the SSCC values had decreased from the wet season to

205 the dry season. In that season, the SSCC value in the Bangka Strait waters only ranged from  
 206 0.16-10 mg/m<sup>3</sup> with an average of 1.5-4.3 mg/m<sup>3</sup> (Fig. 5). Their distribution pattern appears to  
 207 have the same, but the values were lower.



208 **Fig. 4.** The maps of SSCC distribution: a) Wet Season (December-February); b) Transitional  
 209 Season I (March-May); c) Dry Season (June-August); d) Transitional Season II  
 210 (September-November)  
 211

212 In the wet season and transition season I, the SSCC mean values were around 5.0 mg/m<sup>3</sup>  
 213 and 6.4 mg/m<sup>3</sup>, respectively (Fig. 5). By entering the dry season and transition season II, their  
 214 values were decreasing, and the lowest SSCC value occurred in transition season II. The dry  
 215 season commonly represents less precipitation, available sunlight intensity, higher air  
 216 temperature, high phosphate and nitrate concentration (Sidabutar et al., 2020). The highest  
 217 SSCC values occurred during transition season I, which was likely due to rainfall, light  
 218 intensity, and nutrient concentration at optimal conditions for phytoplankton growth.



219

220  
221  
222

**Fig. 5.** Graph of fluctuation in the average distribution of sea surface chlorophyll-a concentration (SSCC) in the waters of the Bangka Strait.

223

224

225

226

227

228

229

230

231

232

233

234

The SSCC values depend on differences in rainfall, light intensity, river run-off, wind, current, and salinity at optimal conditions for plankton growth during this season (Katara et al., 2008; Navarro et al., 2006; Nurdin et al., 2015). In this study, the rainfall, light intensity, river run-off, current, and salinity were the main factors thought to influence the chlorophyll-a distribution. The highest SSCC values occurred during transition season I, which was likely due to the optimal condition for the phytoplankton photosynthesis. The lower SSCC values are found around the offshore and higher near the coastal areas due to the nutrient sources availability derived from the river estuaries (Harahap et al., 2020; Nurdin et al., 2015). Based on the fertility waters (Pelly et al., 2020; Vollenweider et al., 1998), there were four categories of SSCC values namely Oligotrophic (the SSCC value < 1 mg/m<sup>3</sup>), Mesotrophic (1 mg/m<sup>3</sup> ≤ the SSCC value ≤ 3 mg/m<sup>3</sup>), Eutrophic (3 < the SSCC value ≤ 5 mg/m<sup>3</sup>), and Hypereutrophic (the SSCC value > 5 mg/m<sup>3</sup>). According to that category, the Bangka Strait waters were

235 included in the Eutrophic category (rich in nutrients), except during transition season I included  
236 in the hypereutrophic category (nutrient enrichment in high level and frequently found algal  
237 bloom).

238

### 239 *3.3 Data Validation*

240 MODIS data acquisition in October 2020 and in-situ data taken on 24-28 October 2020 can  
241 be seen in Table 1. The linear regression model for the validation test between the MODIS data  
242 and in-situ data was revealed in the scatter plots (Fig. 6). This  $R^2$  value of the SST regression  
243 model is demonstrating a good model performance ( $0.75 < R^2=0.8215 \leq 0.86$ ) as well as the  
244 RSR value is demonstrating an excellent model performance ( $0 < RSR=0.07 \leq 0.5$ ). For the  
245 SSCC regression model, an excellent model performance is demonstrated by the  $R^2$  value ( $0.86$   
246  $< R^2=0.9031 \leq 1$ ), on the contrary, unsatisfactory based on the RSR value ( $RSR=1.216 > 0.7$ ).

247 The validation results are in line with the previous study in the Red Sea Coastal of Saudi Arabia  
248 (Daqamseh et al., 2019) and a study in the Eastern Indian Ocean (Fitriana et al., 2016b). It's  
249 worth highlighting that lower values were revealed in the in-situ data than in the MODIS data.

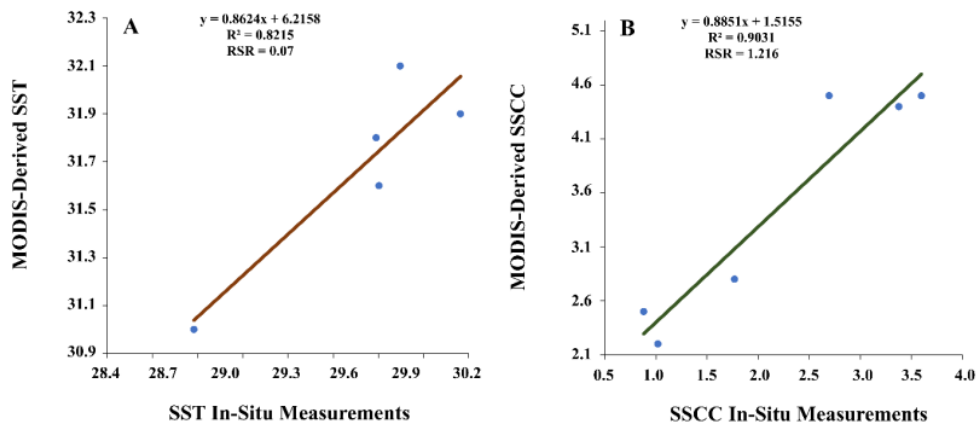
250 This result indicates that the algorithm used to calculate chlorophyll from satellite reflectance  
251 is inadequate, probably due to the optical properties of the water masses (which were affected  
252 hypothetically by terrestrial discharges). This result is an initial identification of PFZ points and  
253 has not validated the PFZ points distribution by using the catch or hydroacoustics data.

254

255 **Table 1**  
 256 Sea Surface Temperature (SST) and Sea Surface Chlorophyll-a Concentration (SSCC).

Stations	Sea Surface Temperature (SST) (°C)		Sea Surface Chlorophyll-a Concentration (SSCC) (mg/m <sup>3</sup> )	
	MODIS Data	In Situ Data	MODIS Data	In Situ Data
	1	31	29.6	4.6
2	31.7	29.2	4.5	0.3
3	31.6	29.6	4.5	2.7
4	31.7	28.5	4.5	3.6
5	31.9	29.1	4.4	3.4
6	32.1	29.7	4.2	1.2
7	31.9	30.0	2.8	1.8
8	31.8	29.6	3.8	0.7
9	31	29.5	2.2	1.0
10	31	28.8	2.5	0.9
Mean	31.6	29.3	3.8	1.6
Stdev.	0.42	0.46	0.94	1.18

257



258

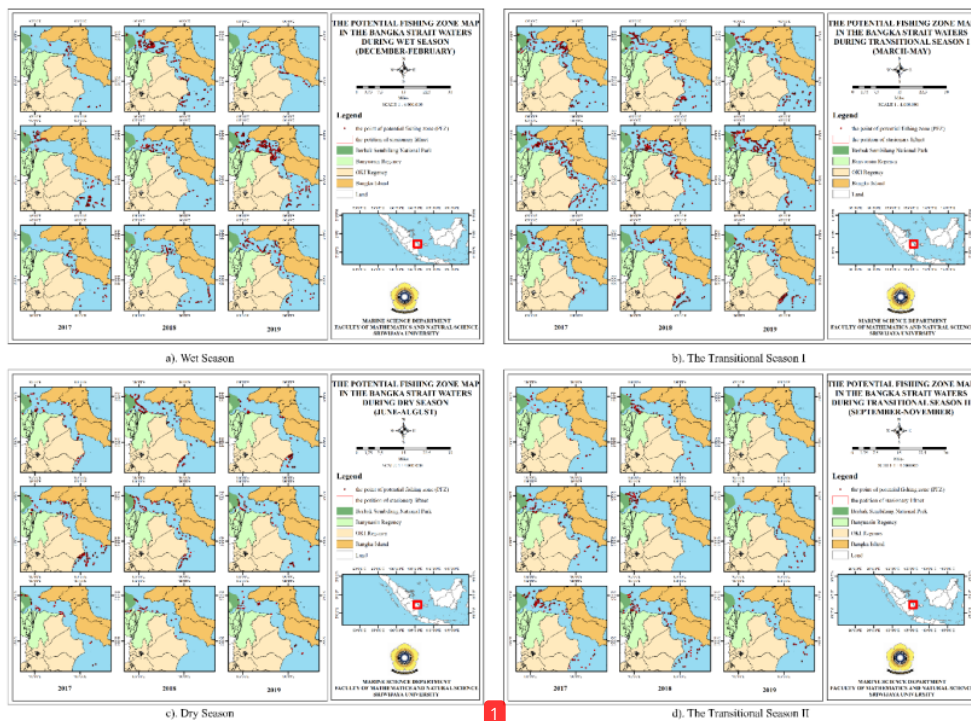
259 **Fig. 6.** Correlation test using the third-order polynomial: a) Sea Surface Temperature (SST);  
 260 b) Sea Surface Chlorophyll-a Concentration (SSCC).  
 261

262 *3.4 The seasonal distribution pattern of the potential fishing zone (PFZ)*

263 The main objective of this study was to identify the SST and SSCC derived from MODIS  
 264 data in determining the PFZs distribution across the Bangka Strait waters. The thermal front  
 265 (SST) dan SSCC data is commonly recognized as the most significant oceanographic factor for  
 266 indicating the natural fish habitat. In this study, SST and SSCC were considered to be shared

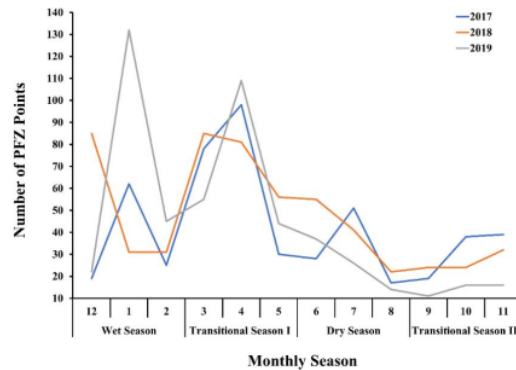
267 a similar influence level over the PFZ mapping. Based on the data validation test (Fig. 6), the  
 268 MODIS data successfully demonstrated excellent model performance in predicting the SST and  
 269 SSCC data.

270 The water zones considered a highly potential fishing ground <sup>2</sup> are assumed to have a large  
 271 amount of available fish stock in consequence of the SST and SSCC aggregation. This is  
 272 because both parameter distributions will affect the fish distribution, fish activity, metabolism,  
 273 and fish nutrients in the sea waters. Some researchers (Devi et al., 2015; Nammalwar et al.,  
 274 2013) stated that the SST and SSCC parameters are also used to indicate fish availability. The  
 275 SST and SSCC parameters were helpful as the key parameters which affect the abundance and  
 276 distribution of *Rastrelliger Kanagurta* in the South China Sea and Makassar Strait of Indonesia  
 277 (Nurdin et al., 2015).



278 **Fig. 7.** The maps of PFZ distribution: a) Wet Season (December-February); b) Transitional  
 279 Season I (March-May); c) Dry Season (June-August); d) Transitional Season II  
 280 (September-November)





282

283 **Fig. 8.** Graph of the amount of PFZ points in the waters of the Bangka Strait

284 The PFZ distribution pattern has been illustrated spatially and temporally (Fig. 7- and 8).  
 285 Fig. 7a demonstrates the distribution pattern of PFZ points (452 PFZ points) in the Bangka  
 286 Strait waters during the wet season for three years. Their distributions in 2017 tend to be  
 287 concentrated near the fishing area of OKI Regency. During 2018, it concentrated on the fishing  
 288 area of the Banyuasin district then moved towards the fishing area of OKI Regency.  
 289 Meanwhile, during 2019 it spread in the Banyuasin and OKI waters and the coastal waters of  
 290 Bangka. Entering transition season I (Fig. 7b), their distribution pattern (636 PFZ points)  
 291 spreads throughout the fishing areas of Banyuasin, OKI, and South Bangka Regencies. During  
 292 three years, it have the same pattern and tends to be dominant spread in the middle to the  
 293 northern waters of the Bangka Strait. Entering the dry season (Fig. 7c), their distribution pattern  
 294 (291 PFZ points) is dominant in many areas of the fishing area of Banyuasin Regency and the  
 295 coastal part of the waters Ogan Komering Ilir Regency, and only a few in the Bangka Regency  
 296 area. Until entering transition season II (Fig.7d), their distribution patterns (219 PFZ points)  
 297 have the same patterns but decrease in the number of PFZ points (Fig. 8). The PFZ points  
 298 numbers were less than the wet season and transition I (Fig. 8) during this season.

299 Overall, the distribution pattern of PFZ points is prominently found more in the northern  
300 part of the Bangka strait and closer to the fishing ground of Stationary lift nets in the Banyuasin  
301 coastal waters. This is because the Banyuasin waters have a high value in SSCC with the  
302 optimum SST, where both parameters were essential for fish growth. The high values of SSCC  
303 are due to several large estuaries as an input of nutrient sources that affect the SSCC values in  
304 these waters. Meanwhile, the fewer points of PFZ in the southern part of the Bangka strait  
305 waters related to the least SSCC values in these waters due to at least in the number of estuaries  
306 as the nutrients sources input for phytoplankton food. Referring illustrated in Figure 8, a  
307 decrease in PFZ points occurred during the dry season and transitional season II when low  
308 rainfall leads to an increase in SST values (Fig.3) and a reduction of SSCC values (Fig. 5). The  
309 results align with the PFZ maps across the Red Sea Coastal of Saudi Arabia (Daqamseh et al.,  
310 2019). The seasonal shifts in both parameters can affect environmental changes that influence  
311 fish aggregation, hence affecting the fish availability in each season (Daqamseh et al., 2019,  
312 2013)

313 The study results demonstrated that integrating the remote sensing and GIS techniques with  
314 statistical validation tests was useful and became a simple method for identifying the PFZ  
315 distribution based on MODIS data. However, validating the PFZ distributions using the catch  
316 data were required. The PFZ can be determined using the SST and SSC derived from satellite  
317 data and can indicate the pelagic fish availability (Devi et al., 2015). Fast and reliable estimation  
318 of the PFZ points possibly supports the fishermen in the effectiveness of fishing time, which  
319 would increase their catch (Nurdin et al., 2015).

#### 320 4. Conclusion

321 The PFZ points were identified based on SSCC and SST data derived from the MODIS  
322 data in this study. The seasonal distribution pattern of the PFZ points from 2017 to 2019  
323 indicated the same pattern in each season and every year. During dry season and transition

324 season II, the PFZ dominated the coastal waters. During the wet season and transition season  
325 I, the PFZ points spread throughout the Bangka Strait waters. Their distribution pattern from  
326 2017-2019 mainly was found around fishing areas in the Banyuasin Regency waters. The PFZ  
327 points were primarily located in transition season I (636 points), while minor PFZ points were  
328 found in transition season II (219 points).

### 329 **3 Declaration of Competing Interest**

330 The authors declare that they have no known competing financial interests or personal  
331 relationships that could have appeared to influence the work reported in this paper.

332

### 333 **Acknowledgment**

334 This work was funded by a grant from the Sriwijaya University and Ministry of Research,  
335 Technology, and Higher Education of the Republic of Indonesia. The authors wish to thank the  
336 anonymous reviewers who significantly improved this paper. And express special appreciation  
337 to the Banyuasin Team 2020, Marine Science Department, and ESAK Laboratory Sriwijaya  
338 University for supporting our research.

### 339 **References**

- 340 Aminot, A., Rey, F., 2001. Chlorophyll a: Determination by spectroscopic methods. ICES Tech.  
341 Mar. Environ. Sci.
- 342 Ardianto, R., Setiawan, A., Hidayat, J.J., Zaky, A.R., 2017. Development of an automated  
343 processing system for potential fishing zone forecast. IOP Conf. Ser. Earth Environ. Sci.  
344 54, 012081. <https://doi.org/10.1088/1755-1315/54/012081>
- 345 Brown, O.B., Minnett, P.J., 1999. MODIS infrared sea surface temperature algorithm,  
346 algorithm theoretical basis document version 2.0, University of Miami.

347 Daqamseh, S.T., Al-Fugara, A., Pradhan, B., Al-Oraiqat, A., Habib, M., 2019. MODIS derived  
348 sea surface salinity, temperature, and chlorophyll-a data for potential fish zone mapping:  
349 West red sea coastal areas, Saudi Arabia. *Sensors* 19, 2069.  
350 <https://doi.org/10.3390/s19092069>

351 Daqamseh, S.T., Mansor, S., Pradhan, B., Billa, L., Mahmud, A.R., 2013. Potential fish habitat  
352 mapping using MODIS-derived sea surface salinity, temperature and chlorophyll-a data:  
353 South China Sea Coastal areas, Malaysia. *Geocarto Int.* 28, 546–560.  
354 <https://doi.org/10.1080/10106049.2012.730065>

355 Devi, G.K., Ganasri, B.P., Dwarakish, G.S., 2015. Applications of Remote Sensing in Satellite  
356 Oceanography: A Review. *Aquat. Procedia* 4, 579–584.  
357 <https://doi.org/10.1016/j.aqpro.2015.02.075>

358 Fauziyah, Agustriani, F., Melda Situmorang, D., Suteja, Y., 2018. Fishing seasons of fish  
359 landed at Sungailiat archipelago fishing port in Bangka Regency. *E3S Web Conf.* 47, 1–  
360 10. <https://doi.org/10.1051/e3sconf/20184706008>

361 Fauziyah, Agustriani, F., Purwiyanto, A.I.S., Putri, W.A.E., Suteja, Y., 2019. Influence of  
362 environmental parameters on the shrimp catch in Banyuasin Influence of environmental  
363 parameters on the shrimp catch in Banyuasin Coastal Water, South Sumatra, Indonesia.  
364 *IOP Conf. Ser. J. Phys. Conf. Ser.* 1282 1282, 012103. [https://doi.org/10.1088/1742-](https://doi.org/10.1088/1742-6596/1282/1/012103)  
365 [6596/1282/1/012103](https://doi.org/10.1088/1742-6596/1282/1/012103)

366 Fauziyah, Purwiyanto, A.I.S., Agustriani, F., Putri, W.A.E., Ermatita, Putra, A., 2020.  
367 Determining the stock status of snapper (*Lutjanus* sp.) using surplus production model: A  
368 case study in Banyuasin coastal waters, South Sumatra, Indonesia. *IOP Conf. Ser. Earth*  
369 *Environ. Sci.* 404, 012009. <https://doi.org/10.1088/1755-1315/404/1/012009>

370 Fitriyah, D., Fahmi, H., Hidayanto, A.N., Arymurthy, A.M., 2016a. A Data Mining Based  
371 Approach for Determining the Potential Fishing Zones. *Int. J. Inf. Educ. Technol.* 6, 187–

372 191. <https://doi.org/10.7763/ijiet.2016.v6.682>

373 Fitriyah, D., Hidayanto, A.N., Gaol, J.L., Fahmi, H., Arymurthy, A.M., 2016b. A Spatio-  
374 Temporal Data-Mining Approach for Identification of Potential Fishing Zones Based on  
375 Oceanographic Characteristics in the Eastern Indian Ocean. *IEEE J. Sel. Top. Appl. Earth*  
376 *Obs. Remote Sens.* 9, 3720–3728. <https://doi.org/10.1109/JSTARS.2015.2492982>

377 Giri, S., Manna, S., Chanda, A., Chowdhury, A., Mukhopadhyay, A., Chakraborty, S., Hazra,  
378 S., 2016. Implementing a spatial model to derive potential fishing zones in the Northern  
379 Bay of Bengal lying adjacent to West Bengal coast, India. *J. Indian Soc. Remote Sens.* 44,  
380 59–66. <https://doi.org/10.1007/s12524-015-0472-2>

381 Guidetti, P., Bussotti, S., Pizzolante, F., Ciccolella, A., 2010. Assessing the potential of an  
382 artisanal fishing co-management in the Marine Protected Area of Torre Guaceto (southern  
383 Adriatic Sea, SE Italy). *Fish. Res.* 101, 180–187.  
384 <https://doi.org/10.1016/j.fishres.2009.10.006>

385 Harahap, S.A., Syamsuddin, M.L., Purba, N.P., 2020. Range of sea surface temperature and  
386 chlorophyll- $\alpha$  values based on mackerel catches in the northern waters of West Java,  
387 Indonesia. *AAFL Bioflux*.

388 Hasyim, B., Hartuti, M., Sulma, S., 2009. Identification of fishery resources in Madura Strait  
389 based on the implementation of potential fishing zone information from remote sensing.  
390 *Int. J. Remote Sens. Earth Sci.* 6, 1–13. <https://doi.org/10.30536/j.ijreses.2009.v6.a1234>

391 Johan, F., Jafri, M.Z., Lim, H.S., Wan Maznah, W.O., 2014. Laboratory measurement:  
392 Chlorophyll-a concentration measurement with acetone method using spectrophotometer,  
393 in: *IEEE International Conference on Industrial Engineering and Engineering*  
394 *Management*. pp. 744–748. <https://doi.org/10.1109/IEEM.2014.7058737>

395 Karuppasamy, S., Ashitha, T.P., Padmanaban, R., Shamsudeen, M., Silva, J.M.N., 2020. A  
396 remote sensing approach to monitor potential fishing zone associated with sea surface

397 temperature and chlorophyll concentration. *Indian J. Geo-Marine Sci.* 49, 1025–1030.

398 Katara, I., Illian, J., Pierce, G.J., Scott, B., Wang, J., 2008. Atmospheric forcing on chlorophyll  
399 concentration in the Mediterranean. *Hydrobiologia* 612, 33–48.  
400 <https://doi.org/10.1007/s10750-008-9492-z>

401 Marini, Y., Setiawan, K.T., 2018. Indonesia sea surface temperature from TRMM Microwave  
402 Imaging (TMI) sensor. *IOP Conf. Ser. Earth Environ. Sci.* 149, 012055.  
403 <https://doi.org/10.1088/1755-1315/149/1/012055>

404 Mustasim, Zainuddin, M., Safruddin, 2015. Thermal and Chlorophyll-a Front in relation to  
405 Skipjack Tuna Catch during the West-East Transition Season, Seram Waters. *J. IPTEK*  
406 *PSP* 2, 294–304.

407 Nammalwar, P., Satheesh, S., Ramesh, R., 2013. Applications of remote sensing in the  
408 validations of Potential Fishing Zones (PFZ) along the coast of North Tamil Nadu, India.  
409 *Indian J. Mar. Sci.* 42, 283–292.

410 Navarro, G., Ruiz, J., Huertas, I.E., Garcia, C.M., Criado-Aldeanueva, F., Echevarria, F., 2006.  
411 Spatial and temporal variability of phytoplankton in the Gulf of Cádiz through remote  
412 sensing images. *Deep. Res. Part II Top. Stud. Oceanogr.* 53, 1241–1260.  
413 <https://doi.org/10.1016/j.dsr2.2006.04.014>

414 Nurdin, S., Mustapha, M.A., Lihan, T., Ghaffar, M.A., 2015. Determination of potential fishing  
415 grounds of *Rastrelliger kanagurta* using satellite remote sensing and GIS technique. *Sains*  
416 *Malaysiana* 44, 225–232. <https://doi.org/10.17576/jsm-2015-4402-09>

417 O'Reilly, J.E., Maritorena, S., Mitchell, B.G., Siegel, D.A., Carder, K.L., Garver, S.A., Kahru,  
418 M., McClain, C., 1998. Ocean color chlorophyll algorithms for SeaWiFS. *J. Geophys. Res.*  
419 *Ocean.* 103, 24937–24953. <https://doi.org/10.1029/98JC02160>

420 O'Reilly, J.E., Mueller, J.L., Chavez, F.P., Strutton, P., Cota, G.F., Carder, K.L., M'uller-  
421 Karger, F., Harding, L., Magnuson, A., Phinney, D., Moore, G.F., Aiken, J., Arrigo, K.R.,

422 Letelier, R., Culver, M., 2000. SeaWiFS postlaunch calibration and validation analyses,  
423 part 3, NASA Technical Memorandum - SeaWiFS Postlaunch Technical Report Series.

424 Pelly, D.A., Marfai, M.A., Pangaribowo, E.H., Fadholi, A., 2020. Chlorophyll-a variability  
425 during positive IOD - The east season period in 2019 in Padang Sea, Indonesia. E3S Web  
426 Conf. 200, 06002. <https://doi.org/10.1051/e3sconf/202020006002>

427 Rajagopal, T., Thangamani, A., Sevarkodiyone, S.P., Sekar, M., Archunan, G., 2010.  
428 Zooplankton diversity and physico-chemical conditions in three perennial ponds of  
429 Virudhunagar district, Tamilnadu. *J. Environ. Biol.* 31, 265–272.

430 Sidabutar, T., Srimariana, E.S., Wouthuyzen, S., 2020. The potential role of eutrophication,  
431 tidal and climatic on the rise of algal bloom phenomenon in Jakarta Bay. *IOP Conf. Ser.*  
432 *Earth Environ. Sci.* 429, 012021. <https://doi.org/10.1088/1755-1315/429/1/012021>

433 Subramanian, S., Manjulekshmi, N., Narendra Pratap, S., Janhavi, K., Tejaswini, P., Pastta,  
434 M.F., 2014. Manual on The use of Potential Fishing Zone (PFZ) forecast. Technical  
435 bulletin No. 40, ICAR Research Complex for Goa (Indian Council of Agricultural  
436 Research), Old Goa – 403 402, Goa, India., Technical bulletin No. 40, ICAR Research  
437 Complex for Goa (Indian Council of Agricultural Research), Old Goa – 403 402, Goa,  
438 India.

439 Suhadha, A.G., Asriningrum, W., 2020. Potential fishing zones estimation based on approach  
440 of area matching between thermal front and mesotrophic area. *J. Ilmu dan Teknol. Kelaut.*  
441 *Trop.* 12, 565–581. <https://doi.org/http://doi.org/10.29244/jitkt.v12i2.28305>

442 Vollenweider, R.A., Giovanardi, F., Montanari, G., Rinaldi, A., 1998. Characterization of the  
443 trophic conditions of marine coastal waters with special reference to the NW Adriatic Sea:  
444 Proposal for a trophic scale, turbidity and generalized water quality index. *Environmetrics*  
445 9, 329–357. [https://doi.org/10.1002/\(SICI\)1099-095X\(199805/06\)9:3<329::AID-  
446 ENV308>3.0.CO;2-9](https://doi.org/10.1002/(SICI)1099-095X(199805/06)9:3<329::AID-ENV308>3.0.CO;2-9)





# Distribution pattern of potential fishing zones in the Bangka Strait Waters: An application of the remote sensing technique

## ORIGINALITY REPORT

6%

SIMILARITY INDEX

3%

INTERNET SOURCES

5%

PUBLICATIONS

1%

STUDENT PAPERS

## PRIMARY SOURCES

- 1 Y P Paulangan, B Barapadang, M A Al. Amin, H Tangkelayuk. "Social-ecological system in Depapre Bay Area of Jayapura Papua Indonesia", IOP Conference Series: Earth and Environmental Science, 2021  
Publication 2%
- 2 [hdl.handle.net](https://hdl.handle.net)  
Internet Source 1%
- 3 [coek.info](https://coek.info)  
Internet Source 1%
- 4 [www.geosafari.org](https://www.geosafari.org)  
Internet Source 1%
- 5 Max Rudolf Muskananfola, Jumsar, Anindya Wirasatriya. "Spatio-temporal distribution of chlorophyll-a concentration, sea surface temperature and wind speed using aqua-modis satellite imagery over the Savu Sea, Indonesia", Remote Sensing Applications: Society and Environment, 2021  
Publication 1%

6

J. Marcello, F. Eugenio, A. Hernandez.  
"Validation of MODIS and AVHRR/3 sea  
surface temperature retrieval algorithms",  
IEEE International IEEE International IEEE  
International Geoscience and Remote Sensing  
Symposium, 2004. IGARSS '04. Proceedings.  
2004, 2004

Publication

1 %

7

[www.coursehero.com](http://www.coursehero.com)

Internet Source

1 %

Exclude quotes On

Exclude matches < 1%

Exclude bibliography On